ECCOMAS Congress 2016
VII European Congress on Computational Methods in Applied Sciences and Engineering
M. Papadrakakis, V. Papadopoulos, G. Stefanou, V. Plevris (eds.)
Crete Island, Greece, 5–10 June 2016

A SEMI-UNSTRUCTURED TURBOMACHINERY MESHING LIBRARY WITH FOCUS ON MODELING OF SPECIFIC GEOMETRICAL FEATURES

Marco Stelldinger[1], **Thomas Giersch**[2], **Felix Figaschewsky**[1], **Arnold Kühhorn**[1]

[1] Chair of Structural Mechanics and Vehicle Vibration Technology
Brandenburg University of Technology Cottbus - Senftenberg
D-03046 Cottbus, Germany
e-mail: marco.stelldinger@b-tu.de

[2] Rolls-Royce Deutschland Ltd & Co KG
D-15827 Blankenfelde-Mahlow, Germany
e-mail: thomas.giersch@rolls-royce.com

Keywords: Semi-unstructured mesh generation, Mesh quality, Turbomachinery, CFD

Abstract. *Computational Fluid Dynamics is widely used for the analysis and the design of turbomachinery blade rows. A well established method is the application of semi-unstructured meshes, that uses a combination of structured meshes in the radial direction and unstructured meshes in the axial as well as the tangential direction. This takes advantage of the approximately two dimensional flow field through the blade rows, whereby a fine radial discretization, excepting the near wall region, is not necessary. Otherwise, it is possible to discretize particular regions, e.g. the leading and trailing edge regions, in the axial and tangential direction without generating unnecessary nodes in the far field. The meshing approach is based on the projection of a two dimensional unstructured mesh defined at a reference surface. Once, the two dimensional mesh is generated the projection is achieved by transfinite interpolation from the reference surface to further radial surfaces using a structured mesh. Due to the modeling of geometrical features, especially fillets, advanced methods for the generation of structured meshes and mesh smoothing algorithms are required.*

The paper presents two different approaches for the generation of an appropriate structured mesh. The first is based on the solution of elliptic partial differential equations. The second approach is based on the split of the domain into fourteen appropriately arranged blocks. Furthermore, two smoothing methods for two dimensional unstructured meshes, a constrained Laplace smoothing and an optimization based approach, are presented. Regarding a more realistic representation of the geometry, methods for the modeling of cavities, variable clearance sizes and fillets are presented. Finally, a comparison of the smoothing techniques applied to a rotor passage is presented and the influence of chosen geometrical features on the flow solution is evaluated.

1 INTRODUCTION

Computational Fluid Dynamics (CFD) is a widely used method for the analysis and the design of aircraft engines. Nowadays, the design process of an aircraft engine based nearly to 90% on CFD simulations [1]. An integral part of CFD simulations is the generation of an appropriate finite volume mesh. This paper is concerned with the mesh generation for the analysis of flows in turbomachinery. Due to the fact, that the computational resources are continuously growing, it is possible to use meshes with a fine grid spacing in CFD simulations. Otherwise, large models are required for specific CFD simulations. These are for instance unsteady forced response analyses, that require the modeling of several blade rows as a full passage, and steady state analyses of an entire high pressure compressor. Hence, it is necessary to generate meshes, that can capture the flow features with good accuracy employing a moderate number of nodes. Another challenge is to generate a mesh, that represents the real geometry as accurately as possible. Thereby, the modeling of specific geometrical features is required. In addition, for multi blade row computations an accurate interpolation of the flow field at the interfaces is required. It is common to generate a finite volume mesh only for a single blade, so that the imposition of periodicity in circumferential direction is mandatory.

Historically, mainly structured hexahedral meshes are used for the discretization of blade passages, since the generation of such meshes is comparatively easy. Structured meshes are obtained either by solving a system of elliptic partial differential equations [2, 3, 4, 5, 6] or by using algebraic approaches [6, 7, 8]. A major disadvantage of such meshes is the generation of unnecessary nodes in the far field, because of required local fine discretization, e.g. at the leading edge and trailing edge of the blade. Another approach is the application of unstructured triangular meshes, primarily used for two dimensional CFD simulations. Such meshes capture flow features of interest, like wake and shock effects, via mesh refinement, without generating unnecessary nodes in the far field. In the three dimensional case the fine resolution at leading edge and trailing edge leads to a large number of nodes in the radial direction. Considering the fact that the flow field in the blade passage is approximately two dimensional a fine resolution in the radial direction is not necessary. Taking into account these facts an alternative and well established method is the application of semi-unstructured meshes, e.g. proposed by Sbardella et al. [9] as well as Kim and Cizmas [10]. This method uses a combination of structured meshes in the radial direction and unstructured meshes in the axial as well as the tangential direction. Furthermore, it is possible to start with a structured O-grid around the blade surface to resolve the boundary layer. Such meshes compose of prismatic and tetrahedral cells and are widely used for viscous CFD simulations, because of a good control of the cell size in the viscous region [11]. They can capture the flow features with good accuracy applying a moderate number of nodes. Another advantage is that only two dimensional meshing algorithms are required. An overview of this strategy is presented in section 2. One part of the generation of semi-unstructured meshes is the projection of a two dimensional unstructured mesh, defined at a two dimensional reference surface, to further surfaces using a two dimensional structured mesh, also denoted as background mesh [10, 12]. In section 3 two approaches for the generation of an appropriate background mesh are presented. The first approach is based on the solution of a system of elliptic partial differential equations. The second approach is based on the split of the domain into fourteen blocks.

In the last years blade geometries became more three dimensional. Thereby, the projected unstructured mesh can be heavily skewed. The modeling of fillets amplifies this effect because the domain of the unstructured mesh constricts near the fillet. This leads to the requirement of

suitable methods to improve the quality of the two dimensional unstructured triangular mesh. In this paper a combination of edge swapping and smoothing is used. In section 4 two smoothing algorithms, a constrained Laplace smoothing and an optimization-based smoothing, are presented. Section 5 presents the modeling of some specific geometrical features, those are cavities, fillets and variable clearance sizes.

2 SEMI-UNSTRUCTURED GRID GENERATION

The geometry of a turbomachinery blade is usually defined as a number of radial sections, defined in cylindrical coordinates by (r, ϑ, x). The radial distribution of these sections must not be confused with the radial distribution of the three dimensional finite volume mesh. Additionally, the position of the inlet, outlet and inner as well as outer casing is usually represented by streamlines, defined in the (x, r) plane. At the beginning, the radial distribution of the mesh has to be defined. E.g. in case of viscous flow simulations a fine radial discretization near the boundaries is necessary. In this paper the definition of the axisymmetric surfaces, that define the radial distribution of the three dimensional mesh, is variable along the machine axis. These fact allows the modeling of clearances of a varying size. Figure 1 shows the radial distribution of a variable stator vane with a constant (a) and a variable clearance size (b).

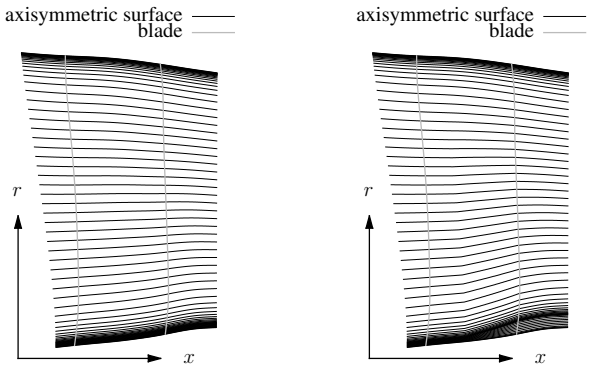

(a) Constant clearance size (b) Variable clearance size

Figure 1: Axisymmetric surfaces, those define the radial distribution of the three dimensional mesh

To apply the implemented mapping procedure the surfaces are defined by two dimensional coordinates (u, v). Applying the two dimensional discrete geometry information the blade surface and the outer boundaries can be defined by linear or cubic splines, see figure 2. The outer boundaries are the inlet, outlet and periodic boundaries. An O-grid is generated around the blade at each spanwise surface. Afterwards an unstructured triangular mesh, that fills the area between the outer boundaries and the boundary of the O-grid, is generated at a chosen reference surface. In this paper the unstructured triangular mesh is generated by applying an advancing front algorithm, that is a widely used method for the generation of unstructured meshes for CFD simulations [9, 13, 14, 15, 16, 17]. The O-grid and the unstructured mesh at the reference surface of a rotor passage are shown in figure 3,

An essential part of the meshing strategy is the projection of the generated unstructured mesh to all spanwise surfaces. In this paper the Transfinite Interpolation (TFI), explained in

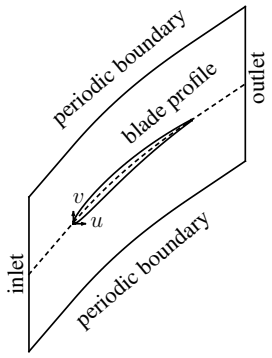

Figure 2: Blade surface and outer boundaries defined in two dimensional coordinates (u, v)

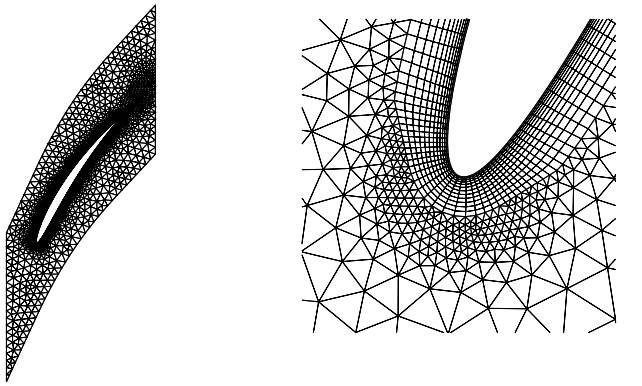

(a) Entire domain (b) Detail of the leading edge

Figure 3: Initial two dimensional mesh of a rotor at the reference surface

section 3, in combination with a background mesh is used. The starting point of the mapping procedure is the generation of appropriate background meshes with identical topology at all spanwise surfaces. Each quadrilateral of the background mesh (figures 6, 7) is represented as an uniform rectangular domain with curvilinear coordinates (ξ, η) applying TFI. In the next step each node i of the unstructured mesh must be located on a quadrilateral j of the corresponding background mesh. Afterwards the coordinates of the node are represented in local curvilinear coordinates (ξ, η) of the corresponding quadrilateral. These coordinates are determined by a Newton-Raphson method, where this process is referred to as inverse mapping. Now the two dimensional coordinates (u, v) of each point i of the unstructured mesh can be obtained at all spanwise surfaces using TFI which is called direct mapping, see figure 4. As a last step the three dimensional grid is obtained by connecting the corresponding points of adjacent spanwise surfaces.

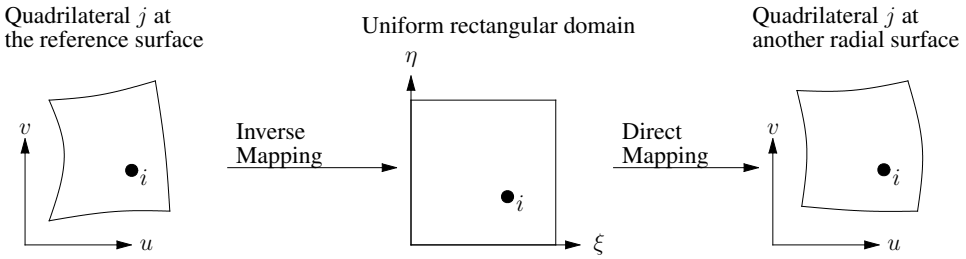

Figure 4: Mapping procedure via Transfinite Interpolation

3 GENERATION OF A BACKGROUND MESH

3.1 Transfinite Interpolation

TFI is a widely used algebraic approach to generate structured meshes and was first described by Gordon [18]. TFI has the advantage to generate grids, these ensure conformity to the boundaries. Thompson et al. [6] give a detailed overview of different interpolation methods used by TFI. In this paper the TFI is not used for mesh generation but entirely for the mapping of quadrilaterals from the physical domain with cartesian coordinates (x, y) into the logical domain with

curvilinear coordinates (ξ, η), as shown in figure 5. The expression for a TFI applying linear interpolation functions, these are used in this paper, is:

$$\begin{aligned}\underline{x}(\xi,\eta) =& \big(1-\eta\big)\underline{x}_s(\xi) + \eta\underline{x}_n(\xi) + \big(1-\xi\big)\underline{x}_w(\eta) + \xi\underline{x}_e(\eta) \\ &- \xi\Big[\big(1-\eta\big)\underline{x}_s(1) + \eta\underline{x}_n(1)\Big] - \big(1-\xi\big)\Big[\big(1-\eta\big)\underline{x}_s(0) + \eta\underline{x}_n(0)\Big] \quad .\end{aligned} \tag{1}$$

Here $\underline{x}_s(\xi)$, $\underline{x}_n(\xi)$, $\underline{x}_w(\eta)$ and $\underline{x}_e(\eta)$ are the boundary curves of the quadrilateral in cartesian coordinates, defined by linear or cubic splines.

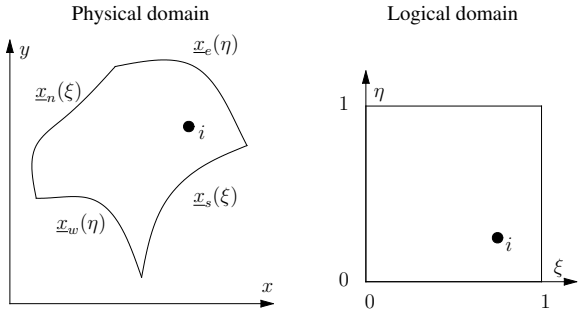

Figure 5: Transfinite Interpolation

3.2 System of elliptic partial differential equations

Solving a system of elliptic partial differential equations is a widely used method to generate structured grids. To obtain an accurate solution, the physical domain is transformed into a uniform rectangular domain by employing a boundary-conforming coordinate transformation. A detailed description is given by Thompson, Thames and Mastin [2, 3, 19]. Consider a system of elliptic partial differential equations in the physical domain (x, y) formulated as a system of Poisson equations:

$$\begin{aligned}\xi_{xx} + \xi_{yy} &= P(\xi,\eta) \\ \eta_{xx} + \eta_{yy} &= Q(\xi,\eta) \quad .\end{aligned} \tag{2}$$

Thereby the curvilinear coordinates (ξ, η) are the solution of the system in the physical domain. The non-homogeneous terms P and Q are the control functions. It is desired to solve the system in the uniform rectangular domain. To formulate the equations (2) into the transformed domain the dependent and independent variables must be interchanged [3]. The equations (2) become

$$\begin{aligned}\alpha x_{\xi\xi} - 2\beta x_{\xi\eta} + \gamma x_{\eta\eta} &= -J^2(\alpha P x_\xi + \gamma Q x_\eta) \\ \alpha y_{\xi\xi} - 2\beta y_{\xi\eta} + \gamma y_{\eta\eta} &= -J^2(\alpha P y_\xi + \gamma Q y_\eta)\end{aligned} \tag{3}$$

where

$$\begin{aligned}\alpha &= x_\eta^2 + y_\eta^2, \quad \beta = x_\xi x_\eta + y_\xi y_\eta \\ \gamma &= x_\xi^2 + y_\xi^2, \quad J = x_\xi y_\eta - x_\eta y_\xi \quad .\end{aligned} \tag{4}$$

The control functions P and Q affect the intersecting angles at the boundaries and the grid spacing. The choice of the control functions has a large influence of the solution on the system.

Some forms of the control functions are proposed by Thompson et al. [3], Thomas and Middlecoff [20] as well as Hsu and Lee [21].

The mapping procedure of section 2 required the generation of a structured mesh in a two dimensional domain, that is located between the outer boundaries of the blade passage and the boundary of the O-grid. Firstly, the surface is divided into four parts, marked by the red lines in figure 6(a). Within these four parts a structured mesh is generated by solving the system of elliptic partial differential equations, that contains suitable control functions. To obtain the solution of the system a Gauss-Seidel method, especially the method of Successive Over Relaxation, is used. A resulting mesh for a rotor domain is shown in figure 6(b).

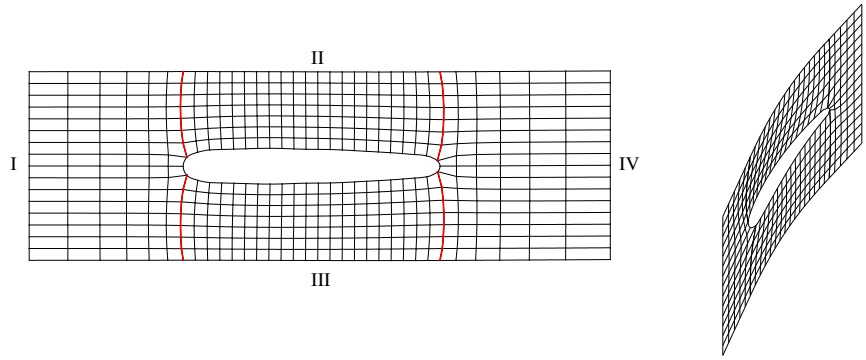

(a) Schematic depiction (b) Rotor domain

Figure 6: Background meshes, generated via solution of elliptic partial differential equations

3.3 Fourteen appropriate arranged blocks

Another way to generate a background mesh is an assembly of fourteen blocks inside the domain. The boundaries of the blocks are defined by linear or cubic splines. Figure 7(a) shows a schematic depiction of the background mesh and figure 7(b) an example for a rotor domain. This kind of background mesh has benefits concerning the computational time for its generation since no system of partial differential equations has to be solved. Furthermore, the inverse mapping procedure requires less time since fewer blocks have to be checked, during the search of the block that contains the regarded node of the unstructured mesh.

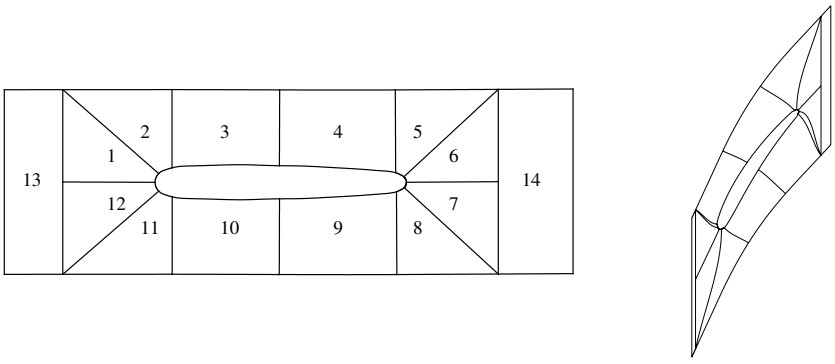

(a) Schematic depiction (b) Rotor domain

Figure 7: Background meshes consisting of fourteen blocks

4 Mesh quality

The mesh quality affects the efficiency and accuracy of CFD simulations. There are many investigations regarding this topic in the literature. Exemplary Katz and Sankaran [22] studied the mesh quality effects on the accuracy of CFD simulations on unstructured meshes by perturbing them randomly. The quality can be improved through several techniques, including point insertion/deletion, edge swapping and mesh smoothing. Canann et al. [23] give a detailed literature review about mesh improvement techniques, especially mesh smoothing. Batdorf et al. [24] use edge swapping as well as mesh smoothing to improve unstructured triangular meshes and performed CFD simulations, that quantify the effect on the solution time and convergence rate. Especially, mesh smoothing algorithms have been shown to be effective in improving the mesh quality. The most common and simplest smoothing technique is the Laplace smoothing. Another common technique is optimization-based smoothing, while it is more computationally expensive than Laplace Smoothing. But it gives better results, especially near concave regions [23]. Freitag [25] as well as Canann et al. [23] studied approaches to combine Laplace and optimization-based smoothing.

Quality measures, also denoted as distortion metrics, are used to determine the quality of a mesh. Stimpson et al give a collection of metrics for evaluating triangles, quadrilaterals, tetrahedra and hexahedra [26]. Amenta et al. [27] represent quality measures especially for triangles. Following Canann et al. [23] the quality measure q for a triangular element can be formulated as follows

$$q = \epsilon \frac{4\sqrt{3}\,A}{l_1^2 + l_2^2 + l_3^2} \quad \text{with} \quad \begin{cases} \epsilon = 1, \text{regular element} \\ \epsilon = -1, \text{inverse element} \end{cases} \tag{5}$$

where A is the area of the triangle and l_1, l_2 and l_3 are the edge lengths. To improve the quality of the unstructured two dimensional mesh a combination of edge swapping and several smoothing techniques is applied. The smoothing techniques are a constrained Laplace smoothing and an optimization-based smoothing.

4.1 Constrained Laplace smoothing

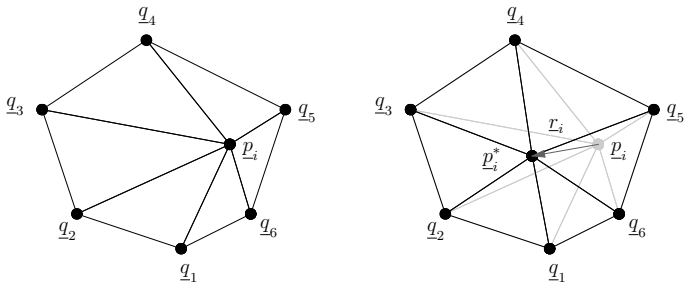

Figure 8: Submesh consisting of six triangular elements

The standard Laplace smoothing is an iterative process, where each node is placed at the average of the adjacent nodes. The left hand side of figure 8 shows a submesh consisting of six triangular elements, where $\underline{p}_i$ is the position vector of the regarded node and $\underline{q}_j$ are the position vectors of the m adjacent nodes. The new position vector $\underline{p}_i^*$ of the regarded node results to

$$\underline{p}_i^* = \frac{1}{m} \sum_{j=1}^{m} \underline{q}_j \quad . \tag{6}$$

It is recommendable to introduce a relaxation factor ω to increase the stability of the smoothing process. The factor should lie within the range $0.0 < \omega < 1.0$. The adapted formula to determine $\underline{p}_i^*$ reads

$$\underline{p}_i^* = \underline{p}_i + \omega \cdot \underline{r}_i \tag{7}$$

where

$$\underline{r}_i = \frac{1}{m} \sum_{j=1}^{m} (\underline{q}_j - \underline{p}_i) \quad . \tag{8}$$

This method usually works quite well for meshes in convex regions, but can results in distorted or inverted elements near concave boundaries [23]. In the flow passage the leading edge and trailing edge of the blade are such concave boundaries. Hence, the constrained Laplace smoothing, that is a variant of the Laplace smoothing, is used. This algorithm relocates the regarded node only if the submesh is improved in terms of a chosen quality measure. The mesh quality of the submesh is defined as the minimum quality q_{min} of the m triangular elements calculated by equation (5):

$$q_{min} = \min_{j \in \{1,\dots,m\}} (q_j) \tag{9}$$

Now the algorithm relocates the regarded node only if $q^*_{min} \geq q_{min}$, where q^*_{min} is the minimum quality obtained by equation 9 if the node would be relocated. To increase the flexibility of the algorithm it is useful to introduce inner iterations n_i within that the relaxation factor ω is halved if $q^*_{min} < q_{min}$. The resulting algorithm is presented for an initial ω of 1.0 in algorithm 1. In some cases, especially near concave boundaries, the constrained Laplace smoothing is unable to improve heavily skewed elements [23]. Hence, it is necessary to use alternative techniques, e.g. optimization-based smoothing to repair these elements.

Algorithm 1 Constrained Laplace smoothing

```
for i = 1, n do
    ω = 1.0
    q_min = min_{j∈{1,...,m}} (q_j)
    r_i = (1/m) Σ_{j=1}^{m} (q_j − p_i)
    for k = 1, n_i do
        p_i^* = p_i + ω · r_i
        q_min^* = min_{j∈{1,...,m}} (q_j^*)
        if q_min^* < q_min then
            ω = ω/2
        else
            exit
        end if
    end for
end for
```

4.2 Optimization-based smoothing

Optimization-based smoothing directly improves the mesh quality, whereby heavily skewed and inverted elements can be improved. Canann et al. [23] give a detailed literature review about existing optimization-based smoothing techniques and distortion metrics. There are global and local optimization techniques, whereby recursive local optimization is the more feasible option [23]. In this paper a local optimization is presented. The goal of the optimization is to determine the new position vector $\underline{p}_i^*$ of the regarded node inside a submesh that maximizes the composite function $f_i(\underline{p}_i)$

$$min(-f_i(\underline{p}_i)) \quad , f_i(\underline{p}_i) = \sigma f_{1,i}(\underline{p}_i) + (1-\sigma) f_{2,i}(\underline{p}_i) \tag{10}$$

where

$$f_{1,i}(\underline{p}_i) = \frac{1}{m}\sum_{j=1}^{m} q_j \quad , f_{2,i}(\underline{p}_i) = min\{q_1, \ldots, q_m\} \quad . \tag{11}$$

Here σ is a relaxation factor and should lie within the range $0.0 < \sigma < 1.0$. The function $f_{1,i}$ conforms to the mean value of the qualities q_j and $f_{2,i}$ is the minimum quality q_j of all concerned triangles. For the investigated turbomachinery meshes $\sigma = 0.0$ has exposed as the most feasible choice. To obtain $min(-f_i(\underline{p}_i))$ a line search strategy in gradient direction is used.

4.3 Application

The outlined smoothing algorithms are applied to improve the mesh of a rotor blade of a high pressure compressor consisting of rather 473 thousand nodes. Figure 9 shows the percentage of triangles, that have a quality measure inside a specific interval, in the non-smoothed mesh and after application of the several smoothing algorithms. In the non-smoothed case it is obvious that some triangles have a really small quality. The smallest quality measure q_{min} is even negative, which signifies the presence of inverse elements. The application of the smoothing algorithms considerably improves the mesh quality. The standard Laplace smoothing as well as the constrained Laplace smoothing lead to a significant reduction of triangles with really small quality. The optimization-based smoothing leads to a minimum quality measure of $q_{min} = 0.59$, while the number of equilateral triangles decreases. Figure 10 shows the distribution of the inner angle ϕ of the triangles within the mesh. The standard Laplace smoothing as well as the constrained Laplace smoothing lead to a reduction of small and large angles. The optimization-based smoothing leads similar to the results of Freitag [25] to more angles in the regions of $45°$ and $90°$, while the number of angels near $60°$ decreases. Table 1 gives an overview of the minimum quality measures q and the minimum as well as the maximum angles ϕ. Additionally, the computational time required for the smoothing process including edge swapping is shown.

	$q_{min}[-]$	$\phi_{min}[°]$	$\phi_{max}[°]$	time $[s]$
no smoothing	-0.02	0.04	179.8	-
Laplace smoothing	0.23	8.6	152.6	4.7
Constr. Laplace smoothing	0.34	12.9	138.3	12.9
Opt.-based smoothing	0.59	23.4	114.5	420.0

Table 1: Results of mesh quality improvement

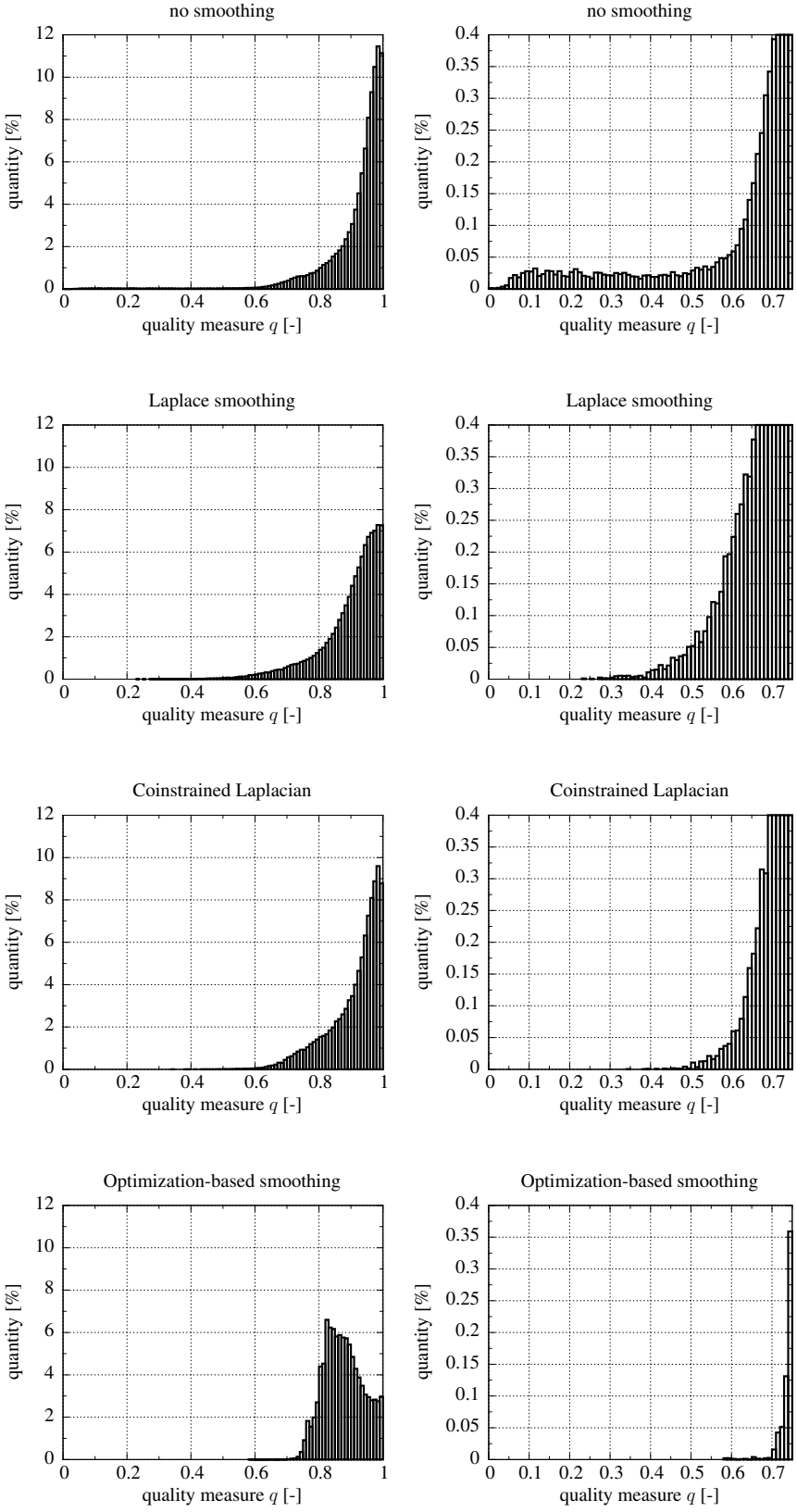

Figure 9: Distribution of quality measures q in a non-smoothed rotor passage and after application of several smoothing techniques

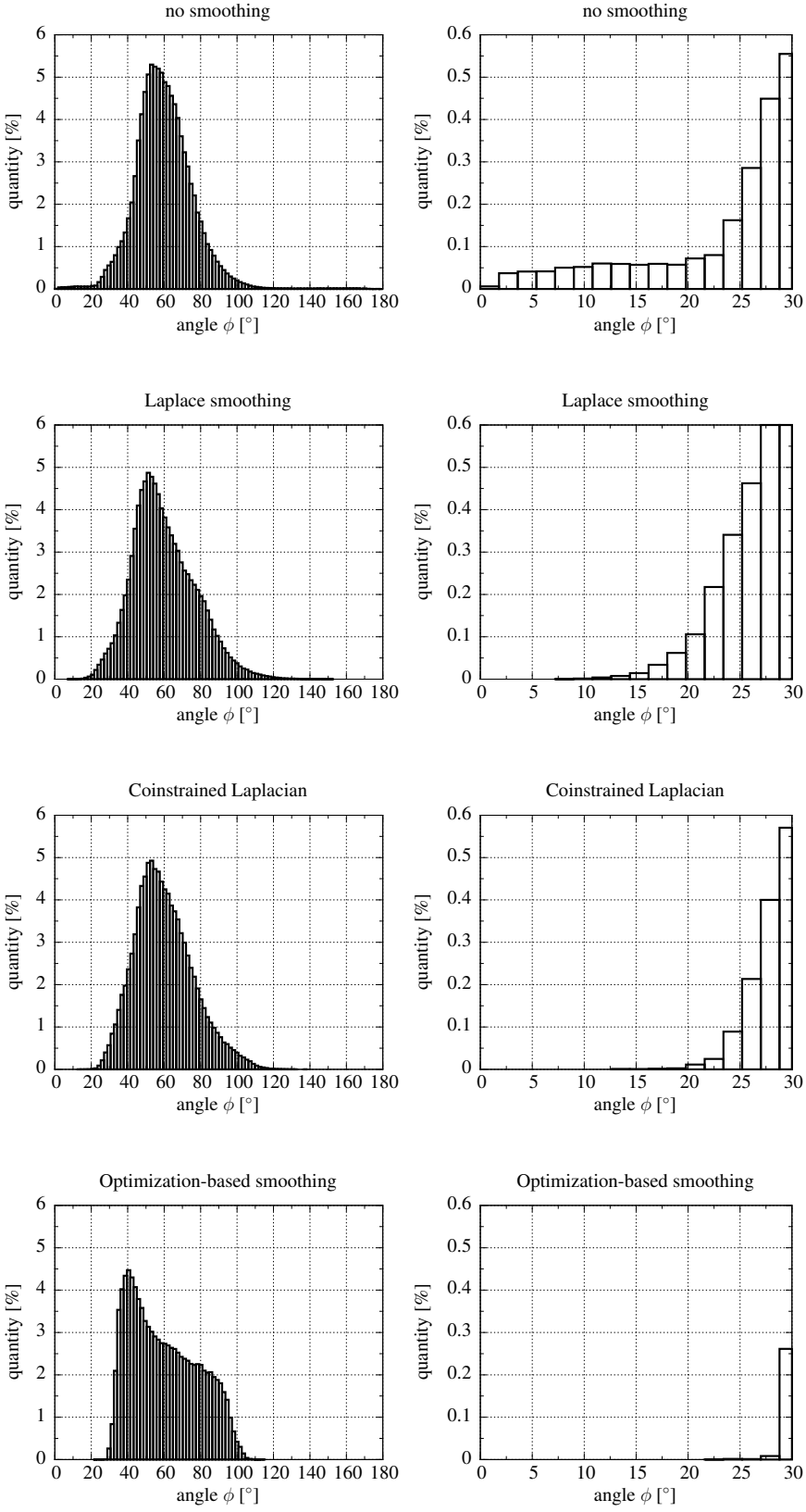

Figure 10: Distribution of angle ϕ in a non-smoothed rotor passage and after application of several smoothing techniques

5 GEOMETRICAL FEATURES

5.1 Modeling of cavities

Traditionally, the flow in turbomachinery blade rows has been simulated using a simplified computational domain consisting of just the blade surface and the main annulus. A more realistic representation of the geometry requires the modeling of cavities and bleed volumes. Burgos et al. [28] presented a method to generate semi-unstructured meshes, especially tailored for the meshing of turbomachinery blade passages and their associated cavities. In this work an analogous method is presented. The geometry of a cavity exhibits a large variation inside the (x, r) plane, while the variation in circumferential direction is usually negligible. Hence, the cavities are meshed in the (x, r) plane using an unstructured triangular mesh, that is extruded in circumferential direction. To connect the three dimensional mesh of the blade passage and the three dimensional mesh of the cavity it is necessary to ensure conformal grids at the interfaces. Since the interface mesh of the cavity has a structured topology, an adaption of the mesh of the blade passage is required. Therefore, a structured mesh at the inlet or outlet is attached. Figure 11(a) shows the structured mesh at the outlet of a stator domain. The figures 11(b,c) show the merged three dimensional mesh of a stator passage including a modeled bleed volume.

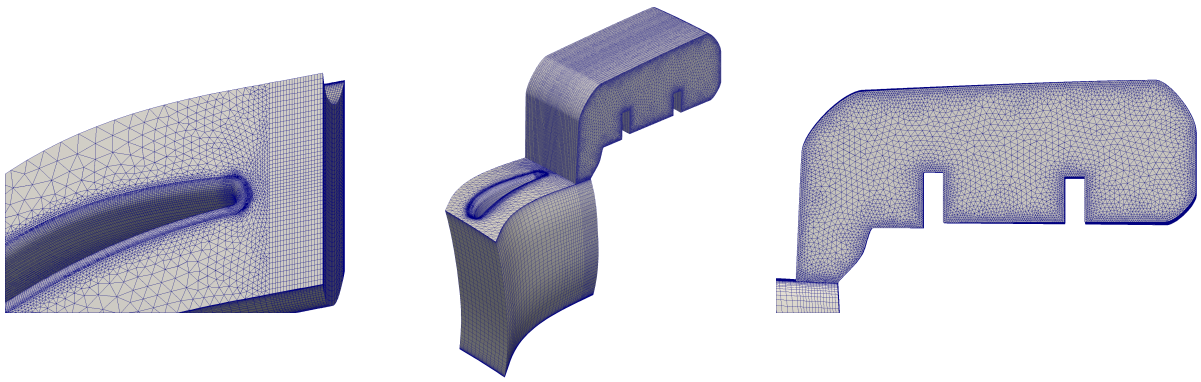

(a) Interface mesh (b) Overall mesh (c) Bleed volume

Figure 11: Modeling of a bleed volume

5.2 Modeling of fillets

The influence of the fillet between the blade and casing on flows in turbomachinery is widely investigated [29, 30, 31, 32, 33]. Zess and Thole [29] performed experimental measurements and CFD simulations, that verified the effectiveness of the leading edge fillet on a gas turbine vane by eliminating the horseshoe vortex. Pieringer and Sanz [30] investigated numerically the influence of the fillet between the blade and casing of a transonic turbine vane on the aerodynamic performance. The results show that considering the fillet in the simulation leads to a significant reduction of mass flow and a change of the specific angular momentum, depending on the flow situation. Furthermore, the efficiency increases when the fillet leads to an attached flow at the fillet and vice versa, decreases when the fillet additionally blocks the flow. Kügeler et al. [31] compared the results of CFD simulations of a 15-stage compressor with measurement data. The study shows differences in the numerical simulation for a geometry model with and without fillets. The fillets decrease flow separations and lead to a different flow behaviour, es-

pecially at the endwalls. This results in a different stage loading, while the overall performance characteristics are similar.

In this work three methods to model blade fillets are presented. Within the first and the second one the topology of the semi-unstructured mesh remains. The blade surface is adapted, while the O-grid is generated as usual. Figure 12(a) shows a plane of the O-grid in normal direction of the blade surface, when no fillet is modeled. Figure 12(b) shows the case, if the fillet is reproduced completely (method 1). This obviously leads to heavily skewed cells near the casing. The heavily skewed cells can be prevented, when the fillet isn't reproduced completely (figure 12(c), method 2). Another method (method 3) to model blade fillets is the application of an alternative mesh topology within the O-grid near the casing. Here the two dimensional structured mesh, that is shown in figure 12(d), is generated by solving a system of elliptic partial differential equations. Figure 13(a) shows the surface meshes of the blades as well as the inner casing near the leading edge of a rotor blade without a fillet. Figure 13(b-d) show the surface meshes, whereas fillets are modeled applying the outlined methods.

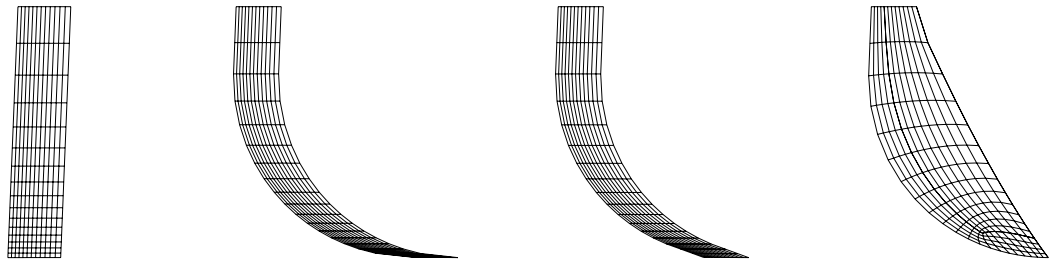

(a) No fillet (b) Method 1 (c) Method 2 (d) Method 3

Figure 12: Implemented methods for fillet modeling

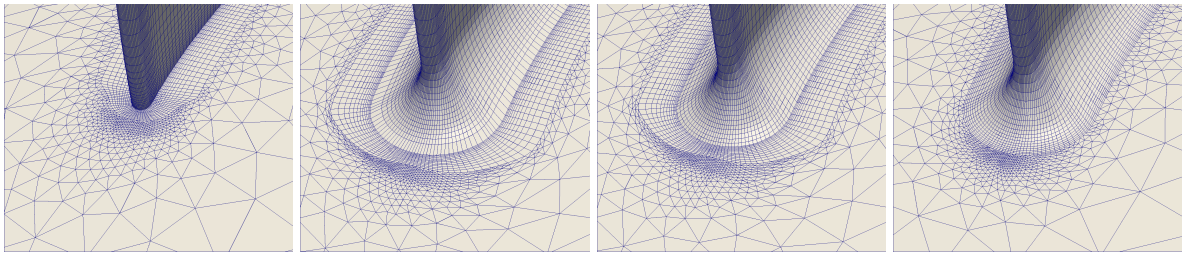

(a) No fillet (b) Method 1 (c) Method 2 (d) Method 3

Figure 13: Mesh at the leading edge of a rotor applying different methods for fillet modeling

Steady state CFD simulations were performed for a rotor passage, using the outlined methods to model a fillet. Figure 14 shows the residuals of the simulations with and without modeled fillet. The model including a fillet, that is modeled by the first method shows a relatively poor convergence rate because of heavily skewed cells near the trailing edge. That fact accords with the investigations of Batdorf et al. [24], that the mesh quality effects the convergence rate. Additionally the attained residual has a relatively poor level. In the other cases the simulations converge to an equal level, while the convergence rates are different.

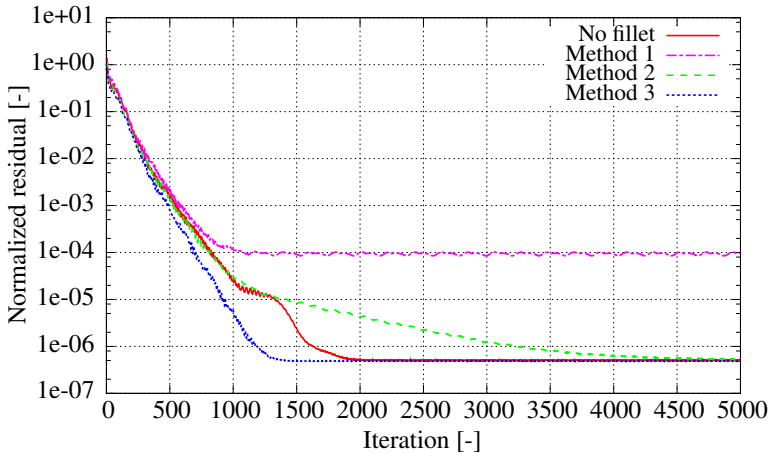

Figure 14: Residuals of steady state simulations applying different methods for fillet generation

5.3 Modeling of variable clearance sizes

Due to a varying stagger angle of variable stator vanes over the speed range of a high pressure compressor, the clearances between the blade and the casing vary too. At the design speed the clearance is approximately constant along the chord length of the blade. If the vanes are closed at part speed the clearances, especially between blade and inner casing, increase from penny to trailing edge. The chosen definition of the axisymmetric surfaces (section 2) allows the modeling of increasing clearances. Figure 15 shows the mesh of a variable stator vane including a constant clearance size between blade and inner casing (red mesh) as well as another one including a varying clearance size (blue mesh).

Steady state CFD simulations were performed for both cases. Due to the pressure difference from the pressure side to the suction side of the blade, the fluid propagates from the pressure side to the suction side through the clearance. Figure 16 shows, that in the case with the constant clearance size, the vortex generated at the suction side is significantly larger than in the other case. This leads to a different flow situation associated with a different pressure field at the blade surface, caused by the several clearance sizes. Consequently, the solution of unsteady CDF simulations, e.g. flutter analyses, can differ noticeable, depending on the modeled geometry.

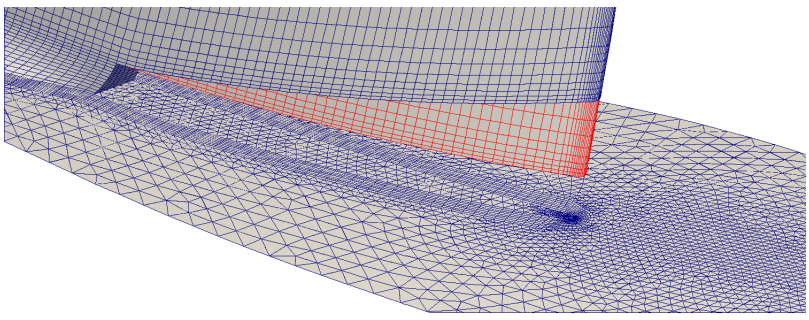

Figure 15: Different modeled clearance sizes of a variable stator vane (blue grid: varying clearance size, red grid: constant clearance size)

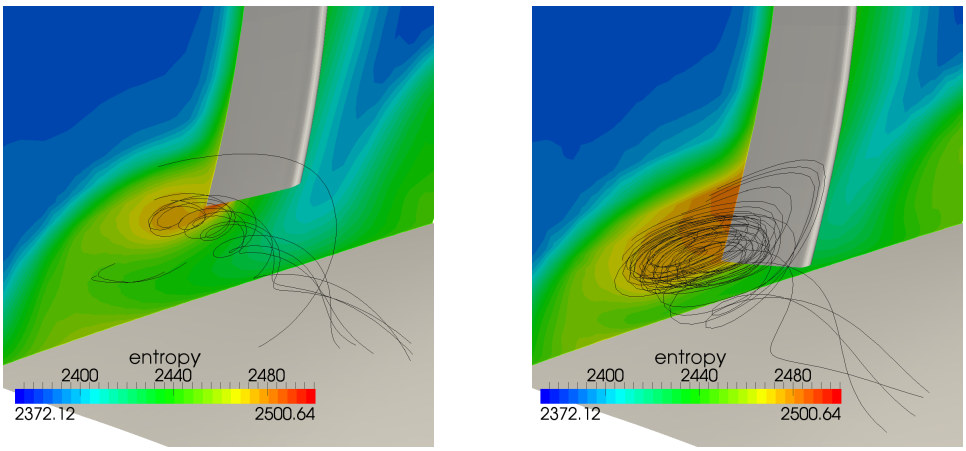

(a) Variable clearance size (b) Constant clearance size

Figure 16: Entropy and streamlines near the trailing edge

6 CONCLUSIONS

In this work a library for turbomachinery meshing was implemented. It enables the generation of semi-unstructured meshes for turbomachinery blade passages, including cavities, fillets and varying clearance sizes. The focus lies on the generation of a mesh, that represents the real geometry as accurately as possible, while the mesh quality is preserved.

Two approaches for the generation of background meshes were presented. The first approach divides the blade passage into four parts. Inside of these parts a structured grid is generated by solving a system of elliptic partial differential equations. The second approach is based on the split of the domain into fourteen blocks. It has benefits concerning computational time towards the first one, because of a faster generation procedure as well as a faster performance of the inverse mapping.

Another key aspect in mesh generation is the improvement of the mesh quality applying suitable methods. Since especially mesh smoothing algorithms have been shown to be effective in improving the mesh quality two smoothing algorithms, a constrained Laplace smoothing and an optimization-based smoothing, were presented. Both algorithms have benefits concerning the achieved mesh quality compared to the standard Laplace smoothing, while the computational time is longer. For the investigated turbomachinery meshes the constrained Laplace smoothing has exposed as the most feasible choice, because of a suitable combination of mesh quality and computational time.

Several methods for the modeling of fillets between blade and the casing were presented. The methods provide meshes with different qualities, that results into different convergence rates and residuals. Furthermore, the axisymmetric surfaces are dependent on the axial position, that enables the modeling of clearances with a variable size. CFD simulations for a variable stator vane with a constant clearance size between blade and inner casing as well as with a variable clearance size were performed. The results show a different flow behaviour near the clearance. This emphasizes the requirement of an accurate representation of the real geometry for CFD simulations of turbomachinery flows.

NOMENCLATURE

Symbols

A	Area of triangular element
f	Composite function
i, j, k	Indices
J	Jacobian
l_1, l_2, l_3	Edge lengths of triangular element
m	Number of adjacent nodes/elements
n	Number of free nodes within the unstructured mesh
n_i	Number of inner iterations (constrained Laplace smoothing)
P, Q	Control functions
q	Quality measure
(u, v)	Local coordinates
(x, y)	Cartesian coordinates (2D)
(r, ϑ, x)	Cylindrical coordinates
α, β, γ	Coefficients (system of elliptic partial equations)
ϵ	sign $(1, -1)$
(ξ, η)	Curvilinear coordinates
σ	Relaxation factor (optimization-based smoothing)
ϕ	Inner angle of triangular element
ω	Relaxation factor (constrained Laplace smoothing)
$\underline{p}$	Position vector of the regarded node
$\underline{q}$	Position vector of the adjacent node
$\underline{r}$	Displacement vector of the regarded node
$\underline{x}$	Vector of cartesian coordinates (x, y)
$\underline{x}_e, \underline{x}_n, \underline{x}_s, \underline{x}_w$	Boundary curves in cartesian coordinates (x, y)

Subscripts/Superscripts

*	Value after smoothing
$_{max}$	Maximum value
$_{min}$	Minimum value

REFERENCES

[1] F. Montomoli, M. Carnevale, A. D'Ammaro, M. Massini, *Uncertainty Quantification in Computational Fluid Dynamics and Aircraft Engines*. Springer, Cham Heidelberg New York Dordrecht London, 2015.

[2] J.F. Thompson, F.C. Thames, C.W. Mastin, *Boundary-Fitted Curvilinear Coordinate Systems for Solution of Partial Differential Equations on Fields Containing Any Number of Arbitrary Two-Dimensional Bodies*. NASA-CR-2729, 1977

[3] J.F. Thompson, F.C. Thames, C.W. Mastin, *TOMCAT—A Code for Numerical Generation of Boundary-Fitted Curvilinear Coordinate Systems on Fields Containing Any Number of Arbitrary Two-Dimensional Bodies*. Journal of Computational Physics, **24**(3), 274-302, Juli 1977

[4] J.L. Steger, R.L. Sorenson, *Automatic Mesh-Point Clustering Near a Boundary in Grid Generation With Elliptic Partial Differential Equations*. Journal of Computational Physics, **33**, 405-410, 1979

[5] J.F. Thompson, Z.U.A. Warsi, C.W. Mastin, *Numerical Grid Generation: Foundations and Applications*. North-Holland, 1985

[6] J.F. Thompson, B.K. Soni, N.P. Weatherill, *Handbook of Grid Generation*. CRC Press, 1999

[7] R.E. Smith, *Algebraic Grid Generation*. Applied Mathematics and Computation, **10-11**, 137-170, 1982

[8] T.I.-P. Shih, R.T. Bailey, H.L. Nguyen, R.J. Roelke, *Algebraic Grid Generation for Complex Geometries*. International Journal for Numerical Methods in Fluids, **13**, 1-31, June 1991

[9] L. Sbardella, A.I. Sayma, M. Imregun, *Semi-Structured Meshes for Axial Turbomachine Blades*. Int. J. Numer. Meth. Fluids, **32**, 569-584, 2000

[10] K. Kim, P.G.A. Cizmas, *Three-Dimensional Hybrid Mesh Generation for Turbomachinery Airfoils*. Journal of propulsion and power, **18**(3), May - June 2002

[11] A. Khawaja, Y. Kallinderis, *Hybrid Grid Generation for Turbomachinery and Aerospace Applications*. Int. J. Numer. Meth. Engng, **49**, 145–166, 2000

[12] M.L. Staten, S.A. Canann and S.J. Owen, *Locating Interior Nodes During Sweeping*. Engineering with Computers, **15**, 212–218, 1999

[13] R. Lohner, P. Parikh, *Generation of Three-Dimensional Unstructured Grids by the Advancing-Front Method*. International Journal of Numerical Methods in Fluids, **8**, 1135-1149, 1988

[14] J. Peraire, J. Peiró, K. Morgan, *Adaptive Remeshing for Three-Dimensional Compressible Flow Computations*. Journal of Computational Physics, **103**(2), 269-285, 1992

[15] S. Pirzadeh, *Unstructured Viscous Grid Generation by Advancing-Front Method*. NASA Constractor Report 191449, 1993

[16] D.J. Mavriplis, *Unstructured Mesh Generation and Adaptivity*. Technical Report ICASE 95-26, 1995

[17] J. Contreras, R. Corral, J. Fernandez-Castañeda, G. Pastor, C. Vasco, *Semi-Unstructured Grid Methods for Turbomachinery Applications*. GT2002-30572, ASME Turbo Expo 2002, Amsterdam, The Netherlands, June 3–6, 2002

[18] W.N. Gordon, C.A. Hall, *Construction of Curvilinear Coordinate Systems and Application to Mesh Generation*. International J. Num. Methods in Eng, **7**, 461-477, 1973

[19] J.F. Thompson, F.C. Thames, C.W. Mastin, *Automatic Numerical Generation of Body-Fitted Curvilinear Coordinate System for Field Containing Any Number of Arbitrary Two-Dimensional Bodies*. Journal of Computational Physics, **15**:3, 299-319, Juli 1974

[20] P.D. Thomas, J.F. Middlecoff, *Direct Control of the Grid Point Distribution in Meshes Generated by Elliptic Equations*. AIAA Journal, **18**, 652-656, 1980

[21] K. Hsu, S.L. Lee, *A Numerical Technique for Two-Dimensional Grid Generation with Grid Control at All of the Boundaries*. Journal of Computational Physics, **96**, 451-469, 1991

[22] A. Katz, V. Sankaran, *Mesh Quality Effects on the Accuracy of CFD Solutions on Unstructured Meshes*. Journal of Computational Physics, **230**, 7670–7686, 2011

[23] S.A. Canann, J.R. Tristano, M.L. Staten, *An Approach to Combined Laplacian and Optimization-Based Smoothing for Triangular, Quadrilateral, and Quad-Dominant Meshes*. 7th International Meshing Roundtable, 479-494, 1998

[24] M. Batdorf, L.A. Freitag, C. Ollivier-Gooch, *Computational Study of the Effect of Unstructured Mesh Quality on Solution Efficiency*. 13th Annual Computational Fluid Dynamics Meeting, Snowmass Village, 1997

[25] L.A. Freitag, *On Combining Laplacian and Optimization-Based Mesh Smoothing Techniques*. Trends in Unstructured Mesh Generation, ASME Applied Mechanics Division, **220**, 37-43, 1997

[26] C. Stimpson, C. Ernst, P. Knupp, P. Pebay, D. Thompson, *The Verdict Geometric Quality Library*. Sandia National Laboratories, 2007

[27] N. Amenta, M. Bern, D. Eppstein, *Optimal Point Placement for Mesh Smoothing*. Journal of Algorithms, **30**(2), 302-322, February 1999

[28] M.A. Burgos, R.Corral, J. Fernández-Castañeda, C. López, *Rapid Meshing of Turbomachinery Rows Using Semi-Unstructured Conformal Grids*. Engineering with Computers, **26**(4), 351-362, 2010

[29] G.A. Zess, K.A. Thole, *Computational Design and Experimental Evaluation of using a Leading Edge Fillet on a Gas Turbine Vane*. ASME Journal of Turbomachinery, **124**, 167-175, 2002

[30] P. Pieringer, W. Sanz, *Influence of the Fillet Between Blade and Casing on the Aerodynamic Performance of a Transonic Turbine Vane*. GT2004-53119, ASME Turbo Expo 2004, Wien, Austria, June 14-17, 2004

[31] E. Kügeler, D. Nürnberger, A.Weber, K. Engel, *Influence of Blade Fillets on the Performance of a 15 Stage Gas Turbine Compressor*. GT2008-50748, ASME Turbo Expo 2008, Berlin, Germany, June 9-13, 2008

[32] L. Castillon, B. Billonnet, S. Péron, C. Benoit, *Numerical Simulations of Technological Effects Encountered on Turbomachinery Configurations with the Chimera Technique*. 27th Congress of International Council of the Aeronautical Sciences, Nice, France, September 19-24, 2010

[33] R. Meyer, S. Schulz, K. Liesner, H. Passrucker, H. Wunderer, *A Parameter Study on the Influence of Fillets on the Compressor Cascade Performance*. Journal of Theoretical and Applied Mechanics, **50**, 131-145, 2012